
THE EVOLUTION OF THE INTERPLAY BETWEEN INPUT DISTRIBUTIONS AND LINEAR REGIONS IN NETWORKS

Xuan Qi

qixuanxd@163.com

Yi Wei

Nanjing University
Nanjing
yui.wyown@gmail.com

ABSTRACT

It is commonly recognized that the expressiveness of deep neural networks is contingent upon a range of factors, encompassing their depth, width, and other relevant considerations. Currently, the practical performance of the majority of deep neural networks remains uncertain. For ReLU (Rectified Linear Unit) networks with piecewise linear activations, the number of linear convex regions serves as a natural metric to gauge the network's expressivity. In this paper, we count the number of linear convex regions in deep neural networks based on ReLU. In particular, we prove that for any one-dimensional input, there exists a minimum threshold for the number of neurons required to express it. We also empirically observe that for the same network, intricate inputs hinder its capacity to express linear regions. Furthermore, we unveil the iterative refinement process of decision boundaries in ReLU networks during training. We aspire for our research to serve as an inspiration for network optimization endeavors and aids in the exploration and analysis of the behaviors exhibited by deep networks.

Keywords Deep neural networks · Input distributions · Linear regions · Piecewise linear activation functions

1 Introduction

In recent years, due to advancements in DNN (Deep Neural Network) structures such as ChannelNets [1], Ghostnets [2], and the development of more effective activation functions such as PReLU [3] and ReLU6 [4], DNNs have achieved remarkable progress in various domains and challenging tasks. Nonetheless, the majority of current networks face the challenge of limited interpretability, making it arduous to comprehend the representation of the input space within these networks. Thus, it becomes imperative to delve into the underlying reasons behind the exceptional performance of networks on various classification tasks. An intuitive research method is to transform networks into the mapping of the input space. DNNs fit a variety of different linear functions by using piecewise linear activation functions (e.g. ReLU). As for the standard networks based on piecewise linear activation, it can transform the input space into different linear regions [5] [6]. Therefore, when the input distribution is two-dimensional, we can obtain a complete correspondence among the linear regions, the input distribution, and the activation states. In fact, networks output classification results by effectively filling these linear regions with linear functions (based on multi-classification).

Fig. 1 shows the intricate linear regions of the ReLU network with a two-dimensional input space for binary classification. Each colored block represents a linear region within the neural network. Moreover, each neuron within the ReLU network divides the input space into two regions along the hyperplane. With the collective contribution of numerous neurons, a region can be further divided into multiple subregions. Consequently, each region encompasses two linear functions to express the output result for the binary classification. The prediction label is determined by selecting the maximum value of the result of two linear functions. As the number of layers increases, the neurons in each layer further partition the regions generated by the previous layer. Fig. 2 shows the progressive arrangement process of linear convex regions in a full-connected ReLU network comprising three hidden layers. Consequently, a network exhibits a multitude of linear regions. These locally dense linear regions serve as a convenient proxy for the local spatial complexity of the network. It should be noted that only a fraction of convex partitions in networks can be characterized

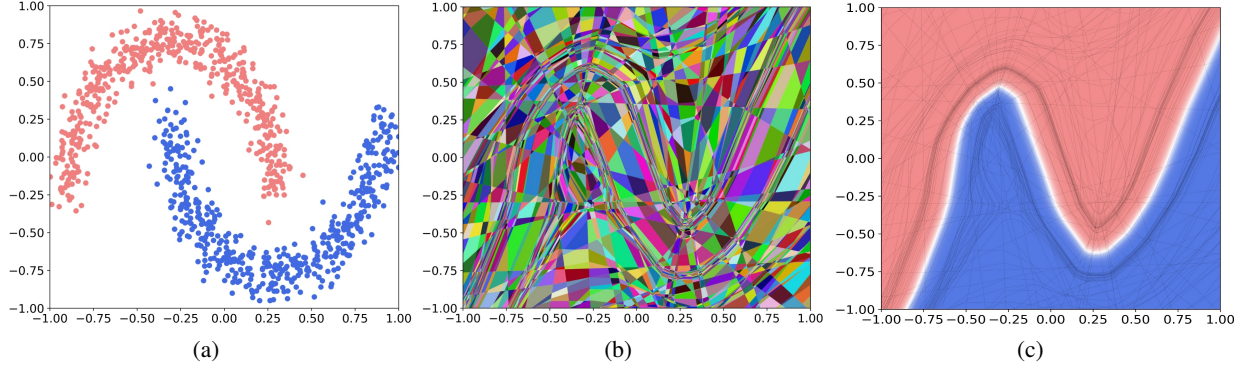


Figure 1: Where are the linear regions and decision boundaries of DNNs? This figure shows the comprehensive correspondence among the linear regions, the input distribution and the activation states within in a fully-connected ReLU network (3 hidden layers, each with 64 neurons.) functioning in a two-dimensional input space during training for 100 epochs. (a) Two-dimensional input dataset "make moons". (b) The visualization of the linear regions, where color blocks represent distinct linear regions of the network. (c) The visualization of the decision regions, where each color represents each type of the input, and the white regions can be regarded as the decision regions approximately.

as the arrangement of hyperplanes. Therefore, we define the arrangement of linear convex regions in networks based on piecewise linear activation as follows:

Definition 1 Let B_g be a collection of G linear convex regions, we have

$$B_g = (B_1^g, \dots, B_{d_g}^g), g \in [G], \quad (1)$$

$$r_g = 1, \dots, d_g, g \in [G], \quad (2)$$

then, the arrangement of these linear convex regions is

$$C(B_1, \dots, B_G), \quad (3)$$

and its regions are

$$\mathbb{E}[\#\{\text{regions in } C\}] = \bigcap_{g=1}^G B_{r_g}^g, (g = 1, \dots, G). \quad (4)$$

In this paper, we conduct a statistical analysis on the number of linear regions in ReLU networks with piecewise linear activation functions. Additionally, we visualize the distributions of these linear regions in a two-dimensional input space. Building upon this, we investigate the relationship between the linear regions and the input distributions in ReLU networks. Our main contributions are summarized as follows:

- (1) For a one-dimensional randomly distributed input, there exists a lower bound on the number of neurons required to express it. It's important to note that this lower bound is determined by the number of linear regions that neurons can express, rather than relying on the theoretical value (see Theorem 1).
- (2) For the same network, our empirical observations indicate that intricate inputs impede its capacity to express linear regions, and this phenomenon is related to the input complexity exceeding the expressive capacity of the network.
- (3) We reveal the evolutionary progression of decision boundaries within ReLU networks during the training process. Furthermore, Our empirical findings suggest that ReLU networks undergo continuous optimization of the decision boundaries during training.

Overall, our findings emphasize the memory capacity of networks operating in a two-dimensional input space when presented with inputs of varying complexity. Furthermore, we partially elucidate the relationship between the operation of ReLU networks and the distribution of inputs. The remainder of this article is organized as follows. Section 2 gives some researchers analysis of the linear regions and operation mechanism of networks. In section 3, we introduce the linear regions of ReLU networks and informally state our theoretical results. Our detailed experimental process is in section 4. In particular, Appendix A provides the proof of Theorem 1, while Appendix B presents our empirical findings.

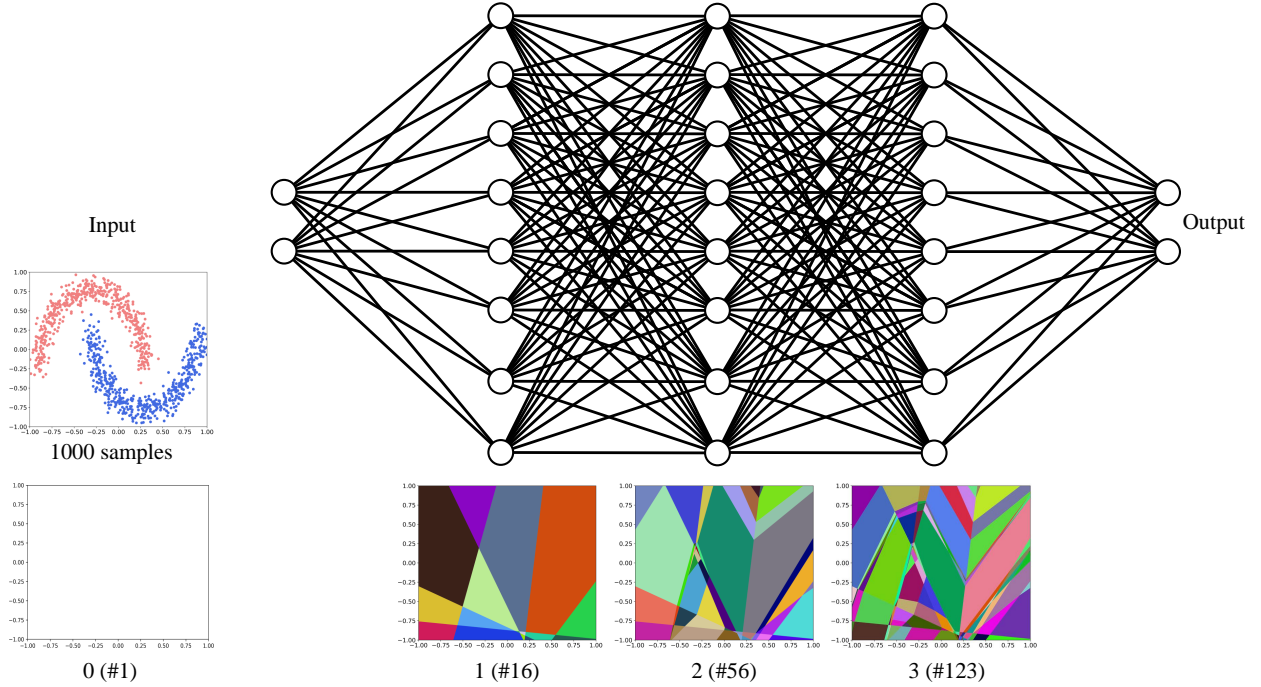


Figure 2: The process of arranging linear convex regions in a fully-connected ReLU network (3 hidden layers, each with 8 neurons,) during training for 100 epochs. We perform a count of the linear regions in each layer. With increasing depth, neurons in each layer combine and segment the linear boundaries inherited from the previous layer, ultimately forming intricate patterns of regions at higher levels. Through this process, the vast number of neurons effectively partitions the input space into numerous distinct regions.

2 Related work

In recent years, a group of researchers has made significant contributions to the analysis of linear regions and the operational mechanisms of networks. The following presents their important contributions in this domain.

2.1 Expressiveness of depth

Regarding the influence of network depth on performance, a study conducted by [7] has shown that for feedforward ReLU networks, changing the depth of the network has a much more significant impact compared to changing the network width, with the impact potentially being exponential. Additionally, [8] analyzed the necessary and sufficient complexity of ReLU networks in depth. In most cases, networks are universal approximators. It has been demonstrated in [9] that deep networks are more efficient than shallow ones. Furthermore, [10] established an upper and lower bound model that can show the complexity of networks in order to study the deep and shallow performance.

2.2 linear regions of networks

In relation to the linear regions of networks, [11] proposed a method to train ReLU networks, enabling the parameters to converge to the global optimum. By partially solving the algebraic topology problem based on ReLU networks, [12] approximately analyzed how initialization affects the number of linear regions. Furthermore, [13] conducted calculations and imposed limitations on linear convex regions to analyze the performance of ReLU networks. Additionally, the works of [14] and [15] delved into studying and establishing bounds on the maximum quantity of linear convex regions generated by ReLU networks.

2.3 Analysis of deep and shallow layers

Several research studies have examined the impact of deep and shallow layers in networks. For instance, the work by [16] delved into the analysis of why networks with a large number of parameters tend to demonstrate superior generalization performance compared to networks with fewer parameters. In a different study, [17] proposed scale normalization methods for networks and investigated the generalization performance of ReLU networks. Taking a physics perspective, [18] explored properties such as symmetry and locality in networks to understand the relationship between deep and shallow layers. Moreover, [19] suggested that conventional methods fail to explain why networks with more parameters typically achieve better generalization performance than those with fewer parameters. Additionally, [20] proposed that shallow sub-networks in ReLU networks have priority in training, and partially explained the operational mechanisms of residual blocks.

3 Linear regions of ReLU networks

This section introduces the properties and definition of linear regions in ReLU networks. Additionally, we introduce informally that there exists a lower bound on the number of neurons that can express any fixed one-dimensional curve in any high-dimensional input, see Theorem 1.

3.1 How to think about linear regions

The ReLU activation function is defined as follows:

$$\text{ReLU}(x) = \max(0, x), \quad (5)$$

when the input x is greater than 0, the output of ReLU function is x . Conversely, when x is less than or equal to 0, the output is 0 and the corresponding node is inactive and does not contribute to the output. During gradient back propagation, the derivative of ReLU is:

$$\text{ReLU}'(x) = \begin{cases} 1, & \text{if } x > 0, \\ 0, & \text{otherwise.} \end{cases} \quad (6)$$

If x is greater than 0, the gradient equals 1; otherwise, the gradient will vanish. Let's consider a fully-connected network with M ReLU layers, and the output of each neuron in each ReLU layer is

$$h^m = \{h_i^m, i \in I^m\}, \quad (7)$$

where I^m is the number of neurons with m layers and m is the number of ReLU layers.

$$h_i^m = (\mathbf{w}_i^m)^T \hat{h}^{m-1} + \mathbf{b}^m, \quad i \in I^m, m \leq M, \quad (8)$$

$$\hat{h}^{m-1} = \max(0, h^{m-1}), \quad (9)$$

where (9) is the result of the previous layer passing through the ReLU activation layer, with \mathbf{b}^m denoting the bias term of the layer m , and \mathbf{w}_i^m signifying the weight of the neurons in the layer m . Therefore, ReLU networks can be expressed as:

$$f(x) = \max(0, \mathbf{w}_M^T \max(0, \mathbf{w}_{M-1}^T \max(0, \dots) + \mathbf{b}^{M-1}) + \mathbf{b}^M), \quad (10)$$

referring to (10), ReLU networks can be regarded as a connected piecewise linear function. Thus, each neuron in the neural network can be expressed as a linear function of input $x \in \mathbb{R}^{n_{in}}$:

$$f_i^m(x) = (\mathbf{A}_i^m)^T x + \mathbf{b}_i^m, \quad i \in I^m, \quad (11)$$

where n_{in} is the dimension of the input, \mathbf{A}_i^m and \mathbf{b}_i^m are the linear weight and bias of the current neuron input.

Therefore, prior to counting the linear regions of a ReLU layer, we establish the input-based linear expression of neurons within the layer. Each linear region is defined by the characteristics of the ReLU activation function, and each linear inequality forms a convex region.

We define the linear regions of ReLU networks as follows:

Definition 2 (adapted from [21]) Let L be a network with input dimension v_{in} and fix η , the trainable parameter vector of L . Define

$$\Phi_L(\eta) := \{x \in \mathbb{R}^{v_{in}} \mid \nabla L(\cdot; \eta) \text{ discontinuity at } x\}, \quad (12)$$

the linear regions of L at η are the connected parts of input without Φ_L :

$$\text{linear regions}(L, \eta) = \{x \mid x \in \mathbb{R}^{v_{in}}, x \notin \Phi_L(\eta)\}, \quad (13)$$

3.2 Bound for expressing one-dimensional inputs

Consider a ReLU network L consisting of p neurons with both input dimension and output dimension 1, which has a simple universal upper bound:

$$\max \#\{\text{regions in } L\} \leq 2^p, \quad (14)$$

where the maximum is over weight values and bias values. The expressiveness of the number of linear regions depends on the width and depth of DNNs. For the influence of depth and width, see [22] and [23].

Theorem 1. (informal). *Let L be a ReLU network with one-dimensional input and output. We assume that the weights and biases are randomly initialized so that the pre-activation $o(x)$ of each neuron q has a bounded average gradient [24]*

$$\mathbb{E}[|\nabla o(x)|] \leq K, \quad \text{some } K > 0, \quad (15)$$

(15) satisfies the independent zero-center weights initialization of the ReLU neural networks with variance as follows:

$$V = \frac{2}{\text{fan-in}}. \quad (16)$$

Then, for each input $S \subset \mathbb{R}$, the subset s_i of S satisfies

$$\{s_i \in S \mid s_{\min} \leq s_i \leq s_{\max}\}. \quad (17)$$

Indeed, s_i is essentially short lines that belong to the line S . According to the above, assuming that the minimum number of linear regions expressing s_i is Q , we obtain the minimum number of neurons q as follows:

$$q \approx \frac{\mathbb{E}[Q]}{|s_i| \cdot c}, \quad (18)$$

where c is the number of breakpoints, for ReLU DNNs, c is equal to 1. This result is also sufficient to calculate the number of neurons along any fixed one-dimensional curve in any high-dimensional input. Referring to (18), we augment the quantity of neurons until the generated linear regions are sufficient to represent the one-dimensional input S . At this juncture, the quantity of linear regions generated by the network can likewise denote the input s_i . Therefore, we obtain the set of neurons that can express the input s_i as follows:

$$\left\{ q \in N^* \mid q \geq \frac{\mathbb{E}[Q]}{|s_i| \cdot c} \right\}. \quad (19)$$

Considering the effect of random weights and biases on each neuron, for any reasonable initialization [24], suppose that the $o(x)$ of q satisfies

$$|o'(x)| = \gamma(1), \quad (20)$$

then, $x \mapsto o(x)$ cannot be highly oscillatory over a large part of q with the input of s_i . Therefore, let the bias be b_q and we have

$$\mathbb{E}[\#\{\text{solutions in } \{o(x) = b_q\}\}] = Z(1), \quad (21)$$

where $Z(1)$ is the solution of the equation we expect. Then, we expect each neuron to generate a fixed quantity of additional linear convex regions. Let the total quantity of additional linear convex regions generated by all neurons be I , referring to (18), we obtain the minimum number of neurons that can express the input s_i under the influence of random weights and biases as follows:

$$q \approx \frac{\mathbb{E}[Q] - I}{|s_i| \cdot c}, \quad (22)$$

referring to (19), similarly, we obtain the set of neurons that can express the input s_i under the influence of random weights and biases as follows:

$$\left\{ q \in N^* \mid q \geq \frac{\mathbb{E}[Q] - I}{|s_i| \cdot c} \right\}. \quad (23)$$

Drawing from the experimental insights presented in [24], we have obtained analogous outcomes (see Fig. 3). We have a great desire to extend our results in subsequent work to calculate a lower bound on the quantity of neurons that can express \mathbb{R} . Additionally, we intend to extend Theorem 1 to spaces of higher dimensions.

4 Experiments

The experimental framework utilized in this study is PyTorch. We represent neurons in each layer of the network as linear functions. In this method, inputs are mapped to neurons to obtain a linear function of each neuron based on the input.

The datasets employed in the experiment consist of two-dimensional data, as it facilitates easy visualization. In reference to [24], the 784-dimensional MNIST dataset was randomly screened for data of two dimensions to visualize and count the linear regions. However, for high-dimensional data, selecting data of two dimensions cannot express the whole dataset well. As a result, this study does not employ such datasets for experimentation and exploration.

We use three distinct two-dimensional datasets, with data values ranging from -1 to 1 . The first dataset is randomly generated data with different samples evenly distributed between -1 and 1 , along with randomly generated labels of either 0 or 1 . The remaining two datasets are "*make moons*" and "*make gaussian quantiles*". Fig. 6 shows the distribution of "*make moons*" and "*make gaussian quantiles*". In addition, we employ the *Adam* optimizer, set the batch size to 32 , and utilize the *Cross Entropy* loss function. In this section, we denote $[n_1, n_2, \dots, n_r]$ to represent the number of hidden layers and neurons, with each hidden layer connected to a ReLU activation layer.

4.1 Linear regions predicated upon one-dimensional input

We compute the count of linear regions for the training examples' lines selected randomly from the origin to the input space. Fig. 3 illustrates the average values of networks $[16, 16, 16]$, $[32, 32, 32]$ and $[64, 64, 64]$, each independently trained ten times. The horizontal axis represents the training epochs, while the vertical axis indicates the ratio of the linear regions count to the number of network neurons. We have obtained results closely resembling those presented in [24]. Namely, throughout the entire training process, the quantity of linear regions does not significantly deviate from the number of neurons in the network, remaining within a constant range. This aligns with the intuitive comprehension described in (18).

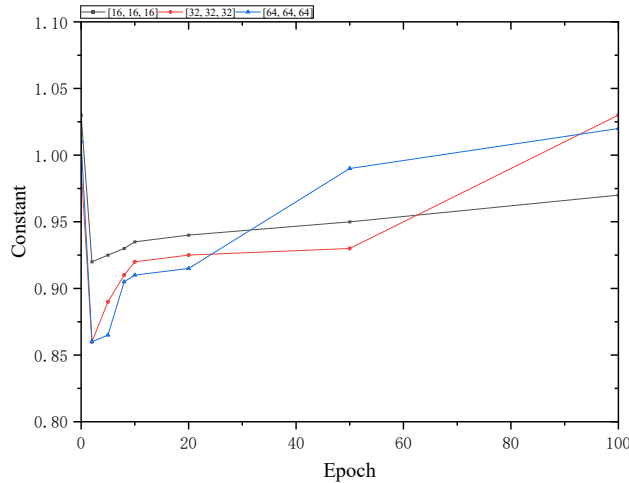


Figure 3: The evolution of the count of linear regions for one-dimensional lines in the input space during the training process of networks $[16, 16, 16]$, $[32, 32, 32]$ and $[64, 64, 64]$ over 100 epochs.

4.2 Linear regions vary with different inputs

We use the network with hidden layers $[32, 32, 32]$ and three ReLU layers. Our random samples are 200, 500, 1000, 2000, 5000 and 10000 respectively.

Fig. 4 and Table 1 show the results of training for 50000 epochs using different random samples and a learning rate of 0.001 . We can find that as the complexity of the sample space increases, the network is capable of segmenting a larger number of linear regions. Based on our experience, this is due to the need for the model to accommodate more irregular and discrete data by employing additional linear regions. However, when the number of samples breaks through a zero bound point, the linear regions will be greatly reduced as depicted in Fig. 4 and Table 1. When the number of samples reaches 2000, the accuracy decreases and the number of linear regions experiences a substantial decline. At

10000 samples, the number of linear regions almost reaches the lowest point. Therefore, our empirical findings suggest that for a network trained on randomly distributed inputs, there exists a critical number of samples that leads to the network's failure in fitting the input. Evidently, this phenomenon is related to the input complexity exceeding the expressive capacity of the network. Fig. 5 shows the linear regions and the visualization results at epoch 50000 for different samples.

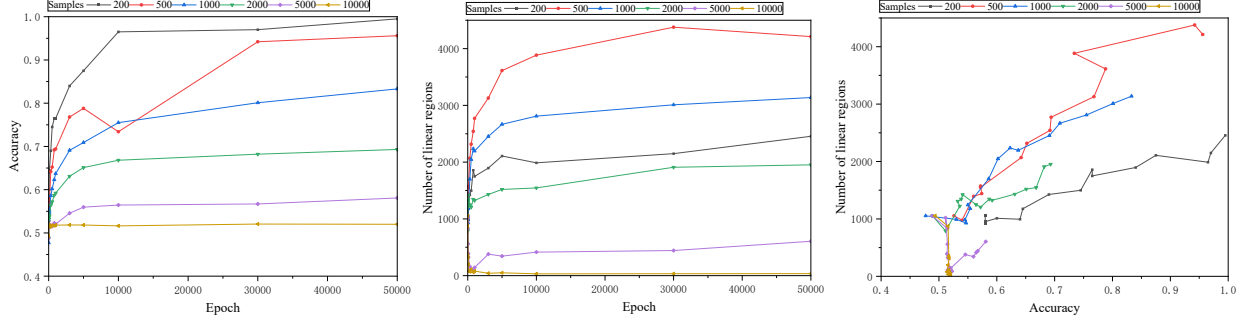


Figure 4: The relationship between the number of linear regions, accuracy, and epochs for random data with varying sample sizes in the network [32, 32, 32].

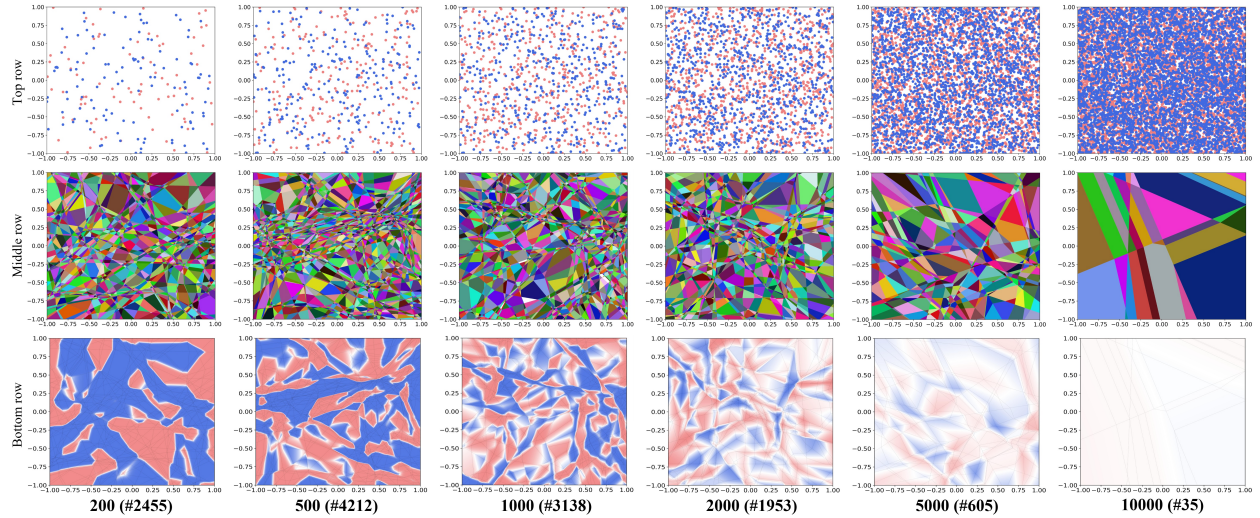


Figure 5: The number of linear regions and the visualization results are presented for random data with varying sample sizes z using the network [32, 32, 32] and training for 50000 epochs, for $z = 200, 500, 1000, 2000, 5000, 10000$. Top row: Random inputs used for training. Middle row: Visualization of the linear regions. Bottom row: Visualization of decision boundaries, where each color represents each type of the input data, and the white regions can be approximately regarded as the decision boundaries.

The experimental results also allow us to obtain the following content. Taking the example of 200 samples, during the optimization process, the network undergoes fine-tuning to fit the data. This fine-tuning process leads to fluctuations in the total number of linear regions within a certain range.

4.3 The process of fitting decision boundaries

We use three different networks, namely [16, 16, 16], [32, 32, 32] and [64, 64, 64]. Each network undergoes training for 100 epochs, and the number of linear regions is recorded. The experimental results for the "make moons" dataset are presented in Fig. 7 and Table 2, while the experimental results for the "make gaussian quantiles" dataset are shown in Fig. 8 and Table 3.

Table 1: The number of linear regions in the network [32, 32, 32] for random data with different samples and epochs.

Epoch \ Samples	0	10	30	50	80	100	300	500	800	1000	3000	5000	10000	30000	50000
200	1151	925	953	1011	995	1176	1426	1499	1858	1749	1896	2108	1988	2149	2455
500	1151	977	1393	1441	1572	1549	2067	2316	2542	2771	3129	3616	3884	4377	4212
1000	1153	992	928	984	1180	1244	1700	2047	2236	2195	2453	2667	2810	3010	3138
2000	1154	791	1222	1308	1344	1423	1250	1205	1346	1324	1431	1519	1545	1910	1953
5000	1151	834	1020	560	391	325	158	111	88	143	379	344	415	442	605
10000	1152	873	353	316	198	79	70	109	61	80	42	51	31	34	35

The three networks exhibit strong memory capacity on both datasets, which differ from random data as they possess a regular structure. The visualization results of decision boundaries for networks with varying numbers of neurons in different epochs are presented in Fig. 9 and Fig. 10 in Appendix B. In these figures, each color corresponds to a specific type of data, and the white regions can be considered as approximate decision boundaries of the networks in their current states. Our empirical findings indicate that during the training process of ReLU networks, the linear regions are continuously optimized until they effectively capture the distribution of the data.

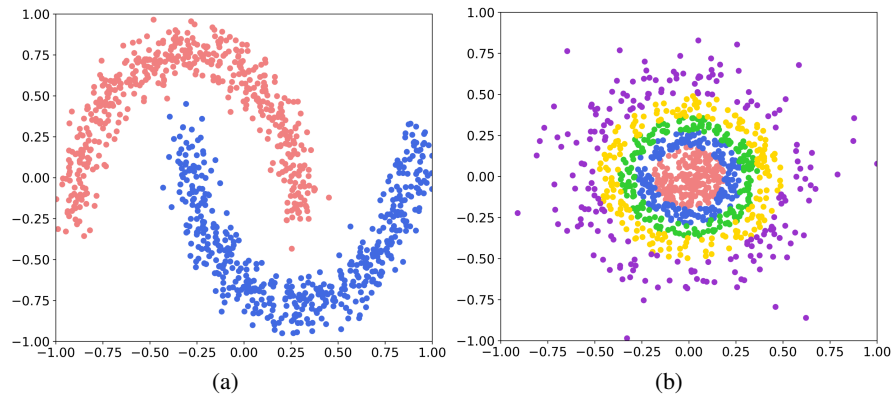


Figure 6: (a) The "make moons" dataset consisting of 1000 samples and 2 classes. (b) The "make gaussian quantiles" dataset consisting of 1000 samples and 5 classes.

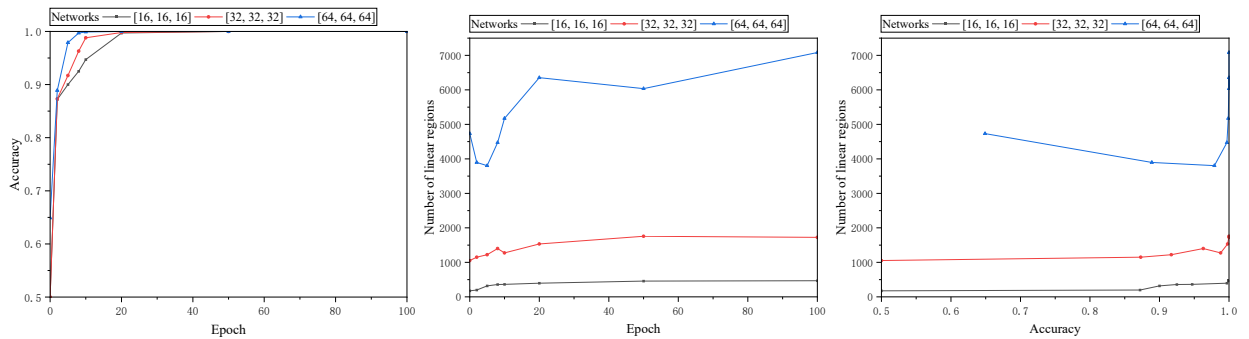


Figure 7: The relationship between the number of linear regions, accuracy and epochs in different networks for the "make moons" dataset with 1000 samples.

Table 2: The number of linear regions in different networks and epochs for the "make moons" dataset with 1000 samples.

Epoch \ DNNs	0	2	5	8	10	20	50	100
[16, 16, 16]	206	198	319	358	363	395	456	467
[32, 32, 32]	1151	1151	1222	1401	1274	1533	1756	1725
[64, 64, 64]	4112	3897	3803	4472	5172	6354	6037	7082

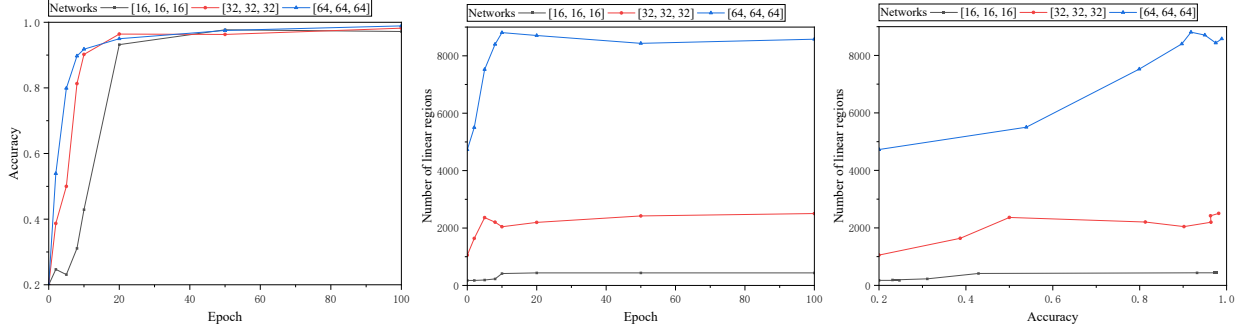


Figure 8: The relationship between the number of linear regions, accuracy and epochs in different networks for the "make gaussian quantiles" dataset with 1000 samples.

Table 3: The number of linear regions in different networks and epochs for the "make gaussian quantiles" dataset with 1000 samples.

Epoch \ DNNs	0	2	5	8	10	20	50	100
[16, 16, 16]	207	174	189	228	415	437	438	436
[32, 32, 32]	1154	1638	2362	2204	2045	2197	2420	2505
[64, 64, 64]	4113	5501	7524	8402	8809	8706	8433	8579

5 Conclusion

In this paper, we have investigated the relationship between linear regions and input distributions in networks based on the piecewise linear activation function ReLU. By computing the number of linear regions in the input space partition of ReLU networks, we have empirically found that complex inputs inhibit the network's ability to express linear regions. In particular, we have demonstrated the existence of a lower bound on the number of neurons required to express any one-dimensional input. Additionally, our two-dimensional visualization results reveal the iterative optimization process of decision boundaries during the training of fully connected ReLU networks. We plan to analyze the relationship between linear regions and input distributions in networks with other architectures in the future.

References

- [1] Hongyang Gao, Zhengyang Wang, Lei Cai, and Shuiwang Ji. Channelnets: Compact and efficient convolutional neural networks via channel-wise convolutions. *IEEE transactions on pattern analysis and machine intelligence*, 43(8):2570–2581, 2021.
- [2] Kai Han, Yunhe Wang, Chang Xu, Jianyuan Guo, Chunjing Xu, Enhua Wu, and Qi Tian. Ghostnets on heterogeneous devices via cheap operations. *International Journal of Computer Vision*, 130(4):1050–1069, 2022.
- [3] Kaiming He, Xiangyu Zhang, Shaoqing Ren, and Jian Sun. Delving deep into rectifiers: Surpassing human-level performance on imagenet classification. In *Proceedings of the IEEE international conference on computer vision*, pages 1026–1034, 2015.

- [4] Andrew G Howard, Menglong Zhu, Bo Chen, Dmitry Kalenichenko, Weijun Wang, Tobias Weyand, Marco Andreetto, and Hartwig Adam. Mobilenets: Efficient convolutional neural networks for mobile vision applications. *arXiv preprint arXiv:1704.04861*, 2017.
- [5] Razvan Pascanu, Guido Montufar, and Yoshua Bengio. On the number of response regions of deep feed forward networks with piece-wise linear activations. *arXiv preprint arXiv:1312.6098*, 2013.
- [6] Guido F Montufar, Razvan Pascanu, Kyunghyun Cho, and Yoshua Bengio. On the number of linear regions of deep neural networks. *Advances in neural information processing systems*, 27, 2014.
- [7] Ronen Eldan and Ohad Shamir. The power of depth for feedforward neural networks. In *Conference on learning theory*, pages 907–940. PMLR, 2016.
- [8] Philipp Petersen and Felix Voigtlaender. Optimal approximation of piecewise smooth functions using deep relu neural networks. *Neural Networks*, 108:296–330, 2018.
- [9] David Rolnick and Max Tegmark. The power of deeper networks for expressing natural functions. *arXiv preprint arXiv:1705.05502*, 2017.
- [10] Dmitry Yarotsky. Error bounds for approximations with deep relu networks. *Neural Networks*, 94:103–114, 2017.
- [11] Raman Arora, Amitabh Basu, Poorya Mianjy, and Anirbit Mukherjee. Understanding deep neural networks with rectified linear units. *arXiv preprint arXiv:1611.01491*, 2016.
- [12] Peter Hinz. Using activation histograms to bound the number of affine regions in relu feed-forward neural networks. *arXiv preprint arXiv:2103.17174*, 2021.
- [13] Qiang Hu, Hao Zhang, Feifei Gao, Chengwen Xing, and Jianping An. Analysis on the number of linear regions of piecewise linear neural networks. *IEEE transactions on neural networks and learning systems*, 33(2):644–653, 2022.
- [14] Hao Chen, Yu Guang Wang, and Huan Xiong. Lower and upper bounds for numbers of linear regions of graph convolutional networks. *arXiv preprint arXiv:2206.00228*, 2022.
- [15] Alexis Goujon, Arian Etemadi, and Michael Unser. The role of depth, width, and activation complexity in the number of linear regions of neural networks. *arXiv preprint arXiv:2206.08615*, 2022.
- [16] Roman Novak, Yasaman Bahri, Daniel A Abolafia, Jeffrey Pennington, and Jascha Sohl-Dickstein. Sensitivity and generalization in neural networks: an empirical study. *arXiv preprint arXiv:1802.08760*, 2018.
- [17] Behnam Neyshabur, Srinadh Bhojanapalli, David McAllester, and Nati Srebro. Exploring generalization in deep learning. *Advances in neural information processing systems*, 30, 2017.
- [18] Henry W Lin, Max Tegmark, and David Rolnick. Why does deep and cheap learning work so well? *Journal of Statistical Physics*, 168(6):1223–1247, 2017.
- [19] Chiyuan Zhang, Samy Bengio, Moritz Hardt, Benjamin Recht, and Oriol Vinyals. Understanding deep learning (still) requires rethinking generalization. *Communications of the ACM*, 64(3):107–115, 2021.
- [20] Tongfeng Sun, Shifei Ding, and Lili Guo. Low-degree term first in resnet, its variants and the whole neural network family. *Neural Networks*, 148:155–165, 2022.
- [21] Boris Hanin and David Rolnick. Deep relu networks have surprisingly few activation patterns. *Advances in neural information processing systems*, 32, 2019.
- [22] Maithra Raghu, Ben Poole, Jon Kleinberg, Surya Ganguli, and Jascha Sohl-Dickstein. On the expressive power of deep neural networks. In *international conference on machine learning*, pages 2847–2854. PMLR, 2017.
- [23] Thiago Serra, Christian Tjandraatmadja, and Srikumar Ramalingam. Bounding and counting linear regions of deep neural networks. In *International Conference on Machine Learning*, pages 4558–4566. PMLR, 2018.
- [24] Boris Hanin and David Rolnick. Complexity of linear regions in deep networks. In *International Conference on Machine Learning*, pages 2596–2604. PMLR, 2019.
- [25] Boris Hanin. Which neural net architectures give rise to exploding and vanishing gradients? *Advances in neural information processing systems*, 31, 2018.

A Proof of Theorem 1

Before proving Theorem 1, we need the conclusion of Theorem 2 from [24].

Theorem 2. (adapted from [24]). Let L be a ReLU network with one-dimensional input and output. We assume that the weights and biases are randomly initialized so that the pre-activation $o(x)$ of each neuron q has a bounded average gradient.

$$\mathbb{E}[\|\nabla o(x)\|] \leq K, \quad \text{some } K > 0, \quad (24)$$

(24) satisfies the independent zero-center weights initialization of the ReLU neural networks with variance as follows:

$$V = \frac{2}{fan-in}. \quad (25)$$

Referring to [25], during ReLU network initialization, each q satisfies

$$\mathbb{E}[\|\nabla o(x)\|^2] = 2. \quad (26)$$

According to the above, suppose that an input subset S of the ReLU network with j neurons, and the average number of linear regions of S is P , we have

$$\mathbb{E}[P] \approx |S| \cdot j \cdot c, \quad S \subset \mathbb{R}, \quad (27)$$

where c is the number of breakpoints, for ReLU networks, c is equal to 1. (27) states that P is proportional to j . This result is also sufficient to calculate the number of linear regions along any fixed one-dimensional curve in any high-dimensional input.

Considering the effect of random weights and biases on each neuron, for any reasonable initialization, suppose that the $o(x)$ of q satisfies

$$|o'(x)| = \gamma(1), \quad (28)$$

referring to (17), $x \mapsto o(x)$ cannot be highly oscillatory over a large part of q with the input of s_i . Therefore, let the bias be b_q and we have

$$\mathbb{E}[\#\{\text{solutions in } \{o(x) = b_q\}\}] = Z(1), \quad (29)$$

where $Z(1)$ is the solution of the equation we expect. Then, we expect each neuron to generate a fixed quantity of additional linear convex regions.

Assuming that the minimum number of linear regions expressing s_i is Q , we obtain the minimum number of neurons q as follows:

(1) For independent zero-center weights initialization, we have

$$q \approx \frac{\mathbb{E}[Q]}{|s_i| \cdot c}, \quad s_i \in S, \quad (30)$$

where c is the number of breakpoints, for ReLU DNNs, c is equal to 1.

(2) Considering the effect of random weights and biases on each neuron, for any reasonable initialization, we have

$$q \approx \frac{\mathbb{E}[Q] - I}{|s_i| \cdot c}, \quad s_i \in S, \quad (31)$$

where c is the number of breakpoints, for ReLU DNNs, c is equal to 1, and I is the quantity of additional linear convex regions generated by all neurons.

Therefore, as we augment the quantity of neurons until the linear regions generated by these neurons are sufficient to represent the one-dimensional input S , we obtain the set of neuron quantities capable of representing s_i as indicated in (19) and (23).

B Visualize the process of fitting decision boundaries

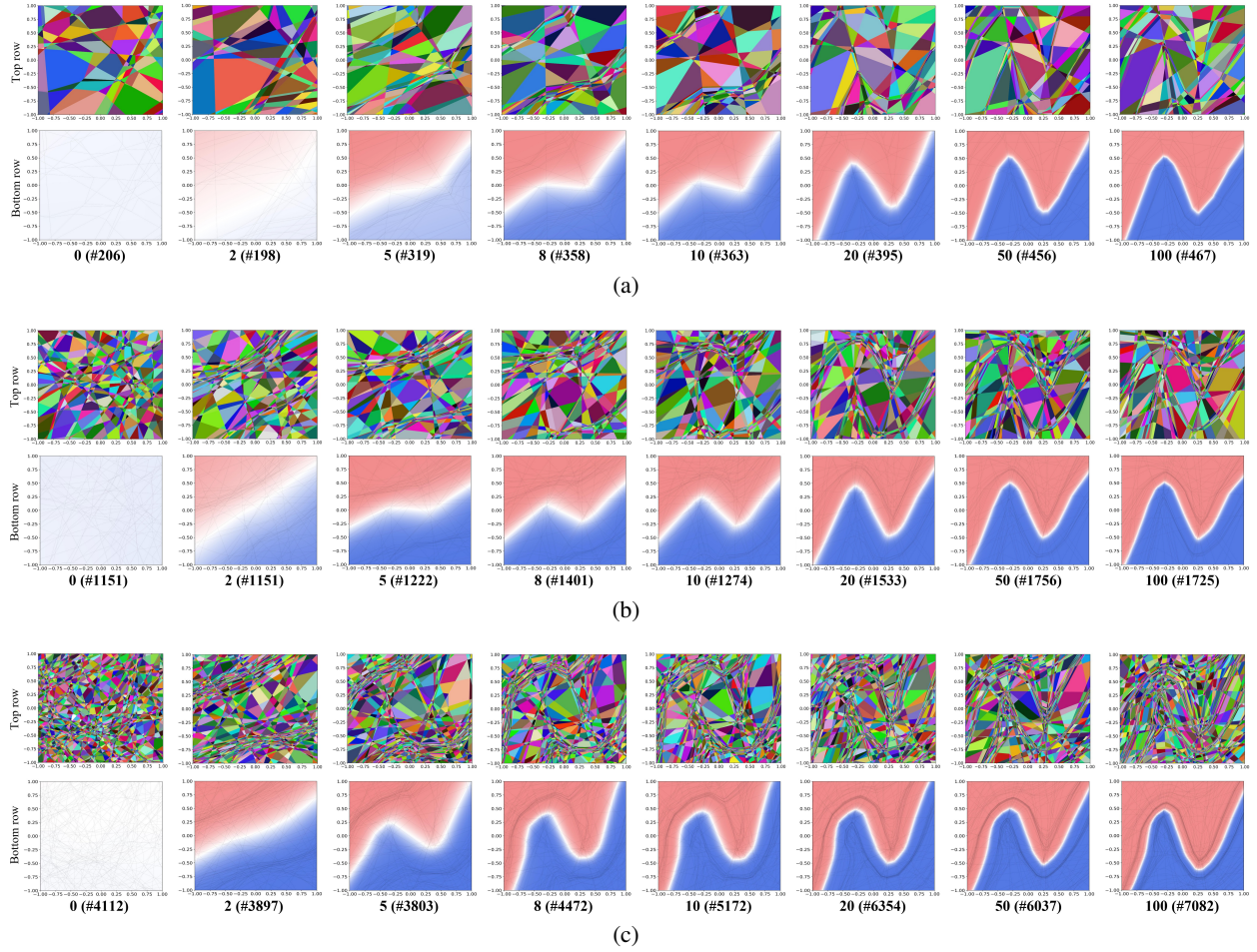


Figure 9: The visualization results and the number of linear regions for different networks trained on the "make moons" at k epochs, for $k = 0, 2, 5, 8, 10, 20, 50, 100$. Top row: Visualization of the linear regions. Bottom row: Visualization of decision boundaries, where each color represents each type of the input data, and the white regions can be approximately regarded as the decision boundaries for the current state of the network. (a) The network [16, 16, 16]. (b) The network [32, 32, 32]. (c) The network [64, 64, 64].

The Evolution of the Interplay Between Input Distributions and Linear Regions

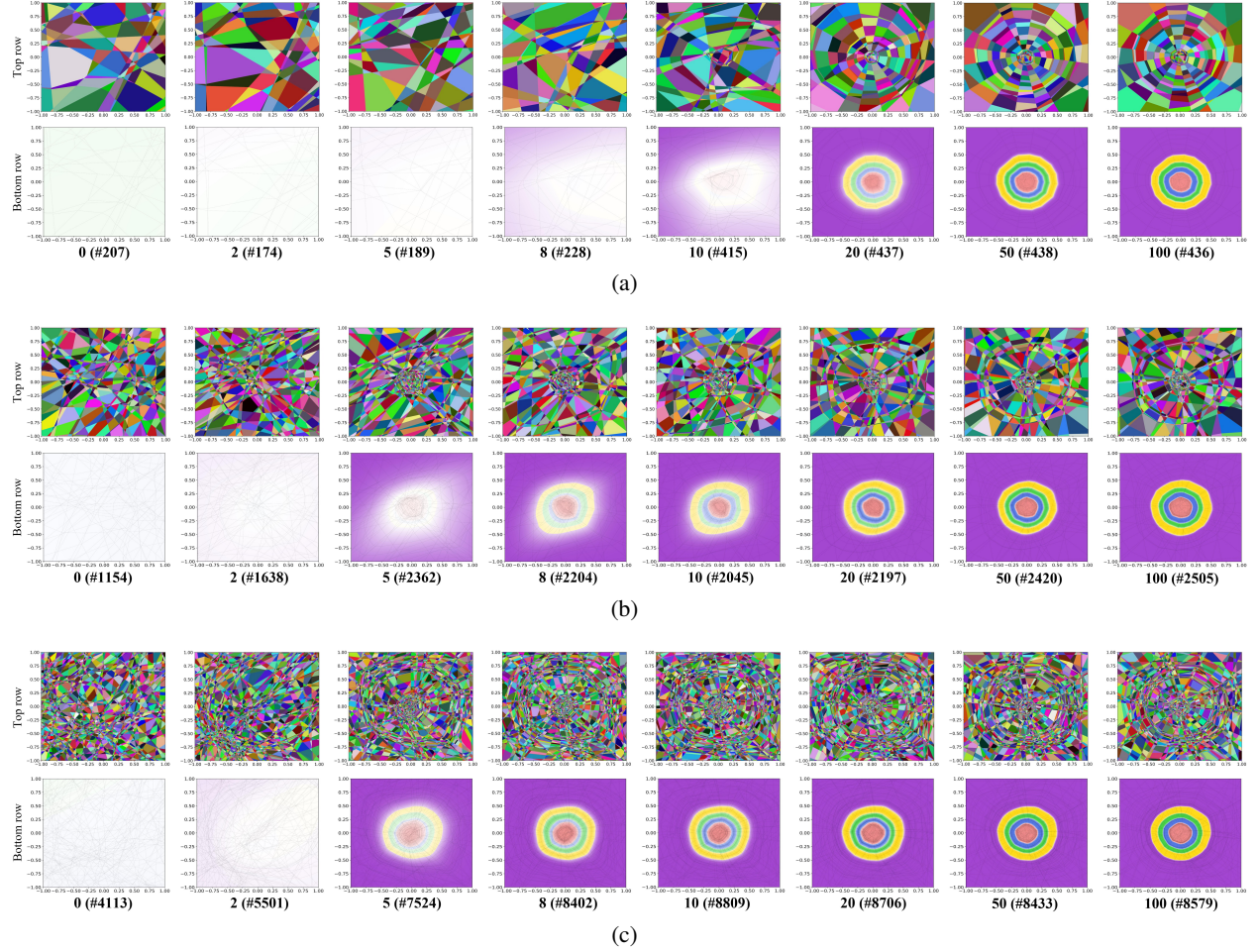


Figure 10: The visualization results and the number of linear regions for different networks trained on the "make gaussian quantiles" at k epochs, for $k = 0, 2, 5, 8, 10, 20, 50, 100$. Top row: Visualization of the linear regions. Bottom row: Visualization of decision boundaries, where each color represents each type of the input data, and the white regions can be approximately regarded as the decision boundaries for the current state of the network. (a) The network [16, 16, 16]. (b) The network [32, 32, 32]. (c) The network [64, 64, 64].